



Scottish Universities Environmental Research Centre

Luminescence Analyses of Samples from Thailand and Laos

April 2019

A.J. Cresswell¹, D.C.W. Sanderson¹, P.A. Carling²

¹ SUERC, East Kilbride, Glasgow

² Geography and Environment, University of Southampton

East Kilbride Glasgow G75 0QF Telephone: 01355 223332 Fax: 01355 229898



The University of Glasgow, charity number SC004401



The University of Edinburgh is a charitable body, registered in Scotland, with registration number SC005336

Summary

Prior investigation of cover sands in Thailand and Vietnam identified two distinct materials present; material containing high sensitivity quartz with robust SAR-OSL luminescence ages $<35\text{ka}$, and material containing lower sensitivity quartz with OSL signals in excess of the $\sim 50\text{ka}$ saturation limit of the SAR method. Thermal transfer methods were developed to extend the range of equivalent dose determination for these older materials. In the work reported here, additional samples of older materials from three sites have been analysed to extend the extent of these observations.

An additional set of profile samples (SUTL3002) and a dating sample (SUTL3003) were collected below the previous samples at Huai Om, Thailand. Laboratory profile measurements give similar sensitivities and apparent doses for quartz grains from the gravel layer to the earlier analyses from the sands immediately above these, with the sandy layer (associated with tektites) and weathered basement samples yielding quartz with even lower sensitivity. The tube sample from immediately above the weathered basement gives an age of $120 \pm 10 \text{ ka}$, slightly older than the sample previously measured immediately above the gravel layer ($95 \pm 15 \text{ ka}$). A sample from the granule layer at Pakse, Laos (SUTL3004) gives an age of $150 \pm 25 \text{ ka}$. A breccia sample from Tad Huakhon, Laos, (SUTL3005) taken from a layer between the basement and a basalt layer gives luminescence sensitivities two orders of magnitude higher than the lower sand and granule layer samples, potentially a result of heating from the lava flow above, and gives an age of $80 \pm 20 \text{ ka}$.

Contents

Summary	i
1. Introduction.....	5
2. Methods.....	7
2.1. Sampling and sample preparation	7
2.2. Portable OSL Measurements	10
2.3. Dating Sample Measurements	11
2.3.1. Water Content	11
2.3.2. Dose Rates	11
2.3.3. Quartz mineral preparation	11
2.3.4. Equivalent dose determination.....	12
3. Results.....	13
3.1. Portable OSL measurements.....	13
3.2. Quartz Single Aliquot Regeneration (SAR) and Dose Extension	15
3.3. Dose Rates	16
4. Discussion	18
5. Conclusions.....	20
References.....	21
Appendix A: Portable OSL and Laboratory Profiling Data.....	24
Appendix B: Dose response curves	26
Appendix C: Dose distributions.....	28

List of figures

Figure 1.1: Locations of luminescence measurements of cover sands in SE Asia from previous work: Khon Kaen (Sanderson et.al. 2001), Kok Yai and Krahad (Porat 2017), Hue (Cresswell et.al. 2018a,b), Kok Yai, Huai Om and Sa Kaeo (Cresswell et.al. 2019). This work reports analyses of samples from Huai Om, Pakse and Tad Huakhon.	6
Figure 2.1: Huai Om section showing the 19 profile samples (dark blue) and the single tube sample (red).....	8
Figure 2.2: Sample location for Pakse, with the sample tube driven vertically into granule layer from a cut bench.....	9
Figure 2.3: Tad Huakhon Waterfall sampling of 0.7-1.0m thick breccias layer between sandstone basement and basalt flow.	10

List of tables

Table 2.1: Summary of samples and SUERC laboratory reference codes	7
Table 2.2: Procedure for combining SAR OSL with dose extension.	12
Table 3.1: Quality parameters for OSL SAR measurements to 50 Gy	15
Table 3.2: Quality parameters for dose extension from 50-1000 Gy	15
Table 3.3: Equivalent doses determined for each sample by SAR-OSL and extended dose methods.....	16
Table 3.4: Activity and equivalent concentrations of K, U and Th determined by HRGS.....	16
Table 3.5: Infinite matrix dose rates determined by HRGS and TSBC.....	16
Table 3.6: Effective beta and gamma dose rates following water content correction.	17
Table A.1: Measurements of profile from Huai Om (SUTL3002) using the SUERC Portable OSL instrument.....	24
Table C.1: Mean equivalent doses determined by OSL SAR measurements (0-50Gy), preferred value in bold.	28
Table C.2: Mean equivalent doses determined by TL-ramp measurements (0-1000Gy), preferred value in bold.....	28
Table C.3: Mean equivalent doses determined by ID measurements (0-1000Gy), preferred value in bold.	28
Table C.4: Mean equivalent doses determined by TT-OSL measurements (0-1000Gy), preferred value in bold.	28

1. Introduction

A significant feature of the soils of southeast Asia is a regionally extensive layer of generally sandy material, in some places 5m or more in depth (eg. Nichol&Nichol 2015, Tamura 1992). These layers are observed throughout Vietnam, Cambodia, Laos and Thailand, and also reported from upland areas of Myanmar and Malaysia, and even the Punjab. The origin of this sand layer has been explained as aeolian (loess-like) deposits of late Pleistocene to Holocene age (Boonsener and Tassanasorn, 1983; Sonsuk and Hastings, 1984; Boonsener, 1987, 1991; Hoang Ngoc Ky., 1989, 1994; Udomchoke, 1989; Šibrava, 1993), lacustrine (Dheeradilok, 1987), marine (Nguyen Duc Tam, 1994) or fluvial (De Dapper, 1987) sediments. Bioturbation is known to be relevant to the processes of formation (Williams, 1978; Bishop et al., 1980; Johnson, 1993), and it has been suggested that this layer is a result of termite activity and subsequent degradation of termite mounds (Löffler and Kubiniok, 1991, 1996). Clarification of the cover layer's age and mode of emplacement is a significant issue (Šibrava, 1993).

Luminescence measurements have been shown to have the potential to date and characterise these sand layers. Samples collected from sites in the Khon Kaen area of NE Thailand (Sanderson et.al. 2001) had excellent luminescence properties, with high-luminescence sensitivity quartz producing consistent ages from both Optically Stimulated Luminescence (OSL) and Thermoluminescence (TL), indicating material that had been strongly bleached prior to deposition. Ages down a 2m profile increased from ~10ka to ~35ka, as expected from an aeolian depositional history with a rate of deposition far higher during the colder periods of the last glacial cycle. This conclusion is supported by physical characterisation of materials from this region by Nichol & Nichol (2015). More recently, OSL ages have been derived for the basal layer of these sand deposits in Thailand of 8 and 19ka (Porat 2017). Studies of samples from Hue, Vietnam (Cresswell et.al. 2018a,b), have shown that the corresponding sand layers have significantly lower luminescence sensitivities, with minerals which indicate less bleaching with TL signals registering a residual geological component, and a more complex age-depth relationship. The basal layer of this location shows mixing between material with an age of 14 ± 2 ka and material with an age significantly in excess of 50ka. Further analysis of the older components (Cresswell et.al. 2018b) using thermal transfer approaches indicated that these older components would have ages of 100-125ka, although with evidence that the associated traps may not be stable at environmental temperatures above 25°C. Further analysis of samples from three sites in Thailand (Cresswell et.al. 2019) found that at Huai Om in southeastern Thailand there was a layer of sandy material with lower OSL sensitivity which produce saturated equivalent doses from Single Aliquot Regeneration (SAR) OSL measurements and equivalent doses of ~150Gy from dose extension methods using thermal transfer of charge from deep traps, overlain by sandy material with very much higher OSL sensitivities which appear to correspond to similar sandy materials elsewhere in Thailand with similar luminescence properties and finite SAR-OSL equivalent doses of <35Gy.

In many locations, these cover sands overlay a tektite containing laterite layer (Tamura 1992, Nichol&Nichol 2015; Mizera et.al. 2016). These tektites, known as the Muong Nong type after the initial descriptions from samples collected a few km south of Muong Nong, Laos (Lacroix 1935), have been identified and dated from several locations in the region. For example, samples from Muong Nong gave fission track ages of between 610 and 720ka have been measured (Gentner et.al. 1969), from Kemeraj, Thailand, an age of 670 ± 40 ka (Gentner et.al. 1969), from Phang Daen, Thailand, ages of 700 and 780ka (Fleischer et.al. 1969), from

Kan Luang Dong, Thailand an age of 450ka (Fleischer et.al. 1969), samples from several locations around Khon Kaen give fission track ages of 620-700ka (Tamura 1992). These tektites are considered to be a type of tektite within a range of tektite referred to as Australasian tektites first described by Darwin (1844) from a sample collected in the Darling River Valley in Australia, with other examples collected during the 19th century from Borneo, Malaysia and Java. The extensive strewn field associated with these and subsequent finds extends from southern China to Tasmania, from the east coast of Australia to the Indian Ocean, with an estimated total mass of tektites ranging from 1×10^{11} to 3×10^{13} kg (Schmidt et al., 1993). These tektites are associated with a large meteorite impact 750 to 800ka in Indochina within the border area between Thailand, Laos and Cambodia (eg: Koeberl 1992), although no impact crater has been located, or the coastal waters of Vietnam (e.g., Schnetzler et al., 1988).

The work presented here will extend the studies of luminescence properties and associated ages for cover sands in different locations in SE Asia, with additional samples from Huai Om and samples from two sites in Laos (Figure 1.1).

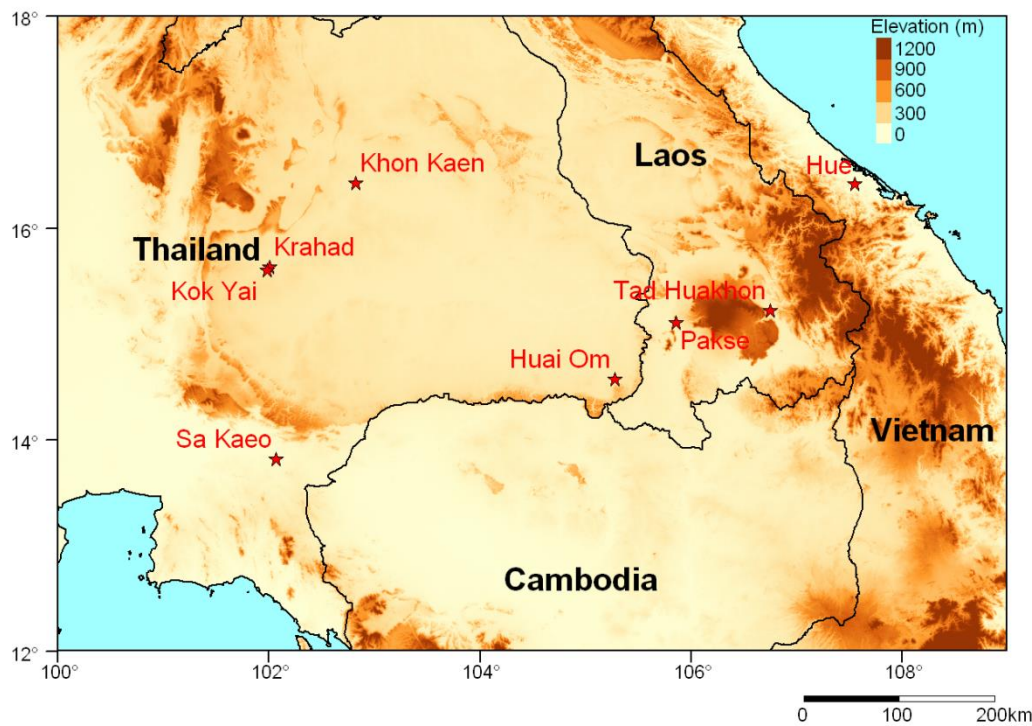


Figure 1.1: Locations of luminescence measurements of cover sands in SE Asia from previous work: Khon Kaen (Sanderson et.al. 2001), Kok Yai and Krahad (Porat 2017), Hue (Cresswell et.al. 2018a,b), Kok Yai, Huai Om and Sa Kaeo (Cresswell et.al. 2019). This work reports analyses of samples from Huai Om, Pakse and Tad Huakhon.

2. Methods

2.1. Sampling and sample preparation

Samples were collected by Paul Carling in March 2019 from three locations; one in Thailand and two in Laos. From Huai Om (Figure 2.1) a profile of 19 stub samples was also collected from a 3.5m high section with one tube sample collected immediately above the weathered basement. The uppermost sample from this profile is from the same stratigraphic context as the lower sample from the earlier profile from this location (Cresswell et.al. 2018b). Although the two profiles are laterally displaced, the nominal depths for these samples have been given such that they're continuous with the earlier profile, with SUTL3002/1 and SUTL2986/1 assigned the same depth. From Pakse (Figure 2.2) a single tube sample was collected from a granule layer within a 2.0m high section of mostly fine sandy-clay to medium sand material, with a pebble base sitting on the weathered basement. From Tad Huakhon Waterfall (Figure 2.3) two blocks of friable breccia were collected from a layer sandwiched between the sandstone basement and an overlying basalt flow. Each sample was given a laboratory (SUTL) reference code upon receipt at SUERC, as summarised in Table 2.1.

Table 2.1: Summary of samples and SUERC laboratory reference codes

SUERC code	Depth (cm)	Description
SUTL3002	19 stub samples and three control samples from Huai Om for environmental profiling. Depths given relative to uppermost sample of SUTL2986	
SUTL3002/1	210	OM+6 (base of cover sand) Equivalent to SUTL2986/1 (OM-1 from 2018 sampling)
SUTL3002/2	220	OM+5 (top of gravel layer)
SUTL3002/3	230	OM+4
SUTL3002/4	240	OM+3
SUTL3002/5	250	OM+2
SUTL3002/6	260	OM+1 (base of gravel layer)
SUTL3002/7	270	OM0 (coarse sand)
SUTL3002/8	280	OM-1 (top of possible ejecta layer)
SUTL3002/9	290	OM-2
SUTL3002/10	300	OM-3
SUTL3002/11	310	OM-4
SUTL3002/12	320	OM-5
SUTL3002/13	330	OM-6
SUTL3002/14	340	OM-7
SUTL3002/15	350	OM-8
SUTL3002/16	360	OM-9
SUTL3002/17	370	OM-10 (base of possible ejecta layer)
SUTL3002/18	380	OM-11 (weathered basement)
SUTL3002/19	390	OM-12 (weathered basement)
SUTL3003	Dating sample from base of possible ejecta layer at Huai Om (between OM-9 and OM-10, SUTL3002/16 and 3002/17)	
SUTL3004	Dating sample from granule layer between two possible ejecta layers at Pakse	
SUTL3005	Breccia blocks from Tad Huakhon Waterfall	



Figure 2.1: Huai Om section showing the 19 profile samples (dark blue) and the single tube sample (red).



Figure 2.2: Sample location for Pakse, with the sample tube driven vertically into granule layer from a cut bench.



Figure 2.3: Tad Huakhon Waterfall sampling of 0.7-1.0m thick breccias layer between sandstone basement and basalt flow.

2.2. Portable OSL Measurements

The profile samples (SUTL3002), excluding the bleached control samples, were appraised using the SUERC portable OSL reader, following an interleaved sequence of system dark count (background), infra-red stimulated luminescence (IRSL) and OSL, similar to that described by Sanderson and Murphy (2010). This method allows for the calculation of IRSL and OSL net signal intensities, depletion indices and IRSL:OSL ratios, which are then used to generate luminescence-depth profiles.

Samples were prepared with duplicate aliquots, by dry sieving to select $<500\mu\text{m}$ grains which were dispensed as a thin layer completely covering 30mm diameter aluminium planchettes which had been sprayed with silicon grease so that the grains adhered to the surface.

Following measurement, the planchettes were placed into a laboratory oven at 350°C for 15 minutes to remove residual luminescence signals, with 1 in 4 planchettes re-measured to confirm adequate zeroing. A ^{90}Sr irradiator was used to add a 5Gy dose to each planchette, and a pre-heat at 110°C for 10 minutes applied to remove unstable components before measurement in the portable OSL reader to determine sensitivity estimates and apparent doses.

2.3. Dating Sample Measurements

The larger dating samples were processed to quantify water content, dose rates and equivalent doses.

2.3.1. Water Content

The tube samples were weighed, saturated with water and re-weighed. Following oven drying at 50°C to constant weight, the actual and saturated water contents were determined as fractions of dry weight. These data were used, together with information on field conditions to determine water contents and an associated water content uncertainty for use in dose rate determination.

2.3.2. Dose Rates

From each of the tube samples, 20 g of the dried material was used in thick source beta counting (TSBC; Sanderson, 1988).

Approximately 150 g of material from each sample was used for environmental dose rate determinations in 125ml polypropylene containers sealed with epoxy resin for high-resolution gamma spectrometry (HRGS). Each sample was stored for 3 weeks prior to measurement to allow equilibration of ^{222}Rn daughters.

2.3.3. Quartz mineral preparation

Approximately 10 g of material was removed for each tube and processed to obtain sand-sized quartz grains for luminescence measurements. Each sample was wet sieved to obtain the 90-150 and 150-250 μm fractions. The 150-250 μm fractions were treated with 1 M hydrochloric acid (HCl) for 10 minutes, 15% hydrofluoric acid (HF) for 10 minutes, and 1 M HCl for a further 10 minutes. The HF-etched sub-samples were then centrifuged in sodium polytungstate solutions of 2.64, and 2.74 g cm^{-3} , to obtain concentrates of feldspars (<2.64 g cm^{-3}) and quartz plus plagioclase (2.64-2.74 g cm^{-3}). Due to very low yields of the lighter fraction this was not separated into different feldspar components by centrifuging this in lighter liquids. The selected quartz fraction was then subjected to further HF and HCl washes (40% HF for 40 mins, followed by 1M HCl for 10 mins).

All materials were dried at 50°C and transferred to Eppendorf tubes. The 40% HF-etched, 2.64-2.74 g cm^{-3} 'quartz' 150-250 μm fractions were dispensed to 10 mm stainless steel discs for measurement. 16 aliquots were dispensed for each sample. The purity of these quartz materials was checked using optical microscopy and a Hitachi S-3400N scanning electron

microscope (SEM), coupled with an Oxford Instruments INCA EDX system, to identify minerals present in an aliquot from each prepared sample.

2.3.4. Equivalent dose determination

A procedure for equivalent dose determination previously used for similar samples (Cresswell et.al. 2019) was used, as summarised in Table 2.2. This is a modified Single Aliquot Regeneration (SAR) procedure to include extended dose measurements. A thermal transfer step, with a TL ramp measurement, isothermal decay and TT-OSL measurement, was included in the natural readout. A standard SAR procedure was then followed to doses of 50 Gy, with higher doses with the thermal transfer steps applied.

Table 2.2: Procedure for combining SAR OSL with dose extension.

Step	Set A	Set B	Set C	Set D
1	Dose (0Gy for natural; regen doses of 10, 20, 30, 40, 50Gy, zero and 10Gy for OSL SAR; regen doses of 50, 100, 200, 500, 1000Gy, zero, & 50Gy for dose extension)			
2 - PH	PH 220°C 10s	PH 240°C 10s	PH 260°C 10s	PH 280°C 10s
3 - OSL	OSL 60s at 125°C (all measurement)			
4 - TL	TL ramp to 260°C (for natural and dose extension)			
5 - ID	Isothermal decay for 30s (for natural and dose extension)			
6 - TTOSL	TT-OSL 60s at 125°C (for natural and dose extension)			
7 - TD	1 Gy Test Dose (for natural and OSL SAR)			
8 - PH	PH 220°C 10s	PH 240°C 10s	PH 260°C 10s	PH 280°C 10s
9 - OSL	OSL 60s at 125°C (for natural and OSL SAR)			
10 - TD	50 Gy Test Dose (for natural and dose extension)			
11 - PH	PH 220°C 10s	PH 240°C 10s	PH 260°C 10s	PH 280°C 10s
12 - OSL	OSL 60s at 125°C (for natural and dose extension)			
13 - TL	TL ramp to 260°C (for natural and dose extension)			
14 - ID	Isothermal decay for 30s (for natural and dose extension)			
15 - TTOSL	TT-OSL 60s at 125°C (for natural and dose extension)			
16	Thermal treatment 350°C 200s (for dose extension)			

3. Results

3.1. Portable OSL measurements

The results of the portable OSL measurements of the natural signals are shown in Fig. 3.1 (and, tabulated in the Appendix Table A.1). These show considerable concordance between the two aliquots of each sample, with small IRSL signals (10^3 - 10^4 counts in 60s) and very much higher OSL signals (10^4 - 10^6 counts in 60s) consistent with quartz rich material. The OSL signals show very high depletion indices, especially for the top two samples in the cover sands and the top of the gravel layer. The OSL front end signal (calculated by subtracting the counts for the second 30s of the measurement from the first 30s) is strongly correlated with the net counts.

The data from the 2018 profile (Cresswell et.al. 2018b) have been included in Fig. 3.1, noting that these were bulk samples presented in a different geometry which could introduce systematic offsets in the measurements. These measurements were all within the cover sand layer, laterally displaced from the current profile, and indicate a higher IRSL and lower OSL contribution and a further order of magnitude increase in OSL intensity further up the stratigraphic sequence.

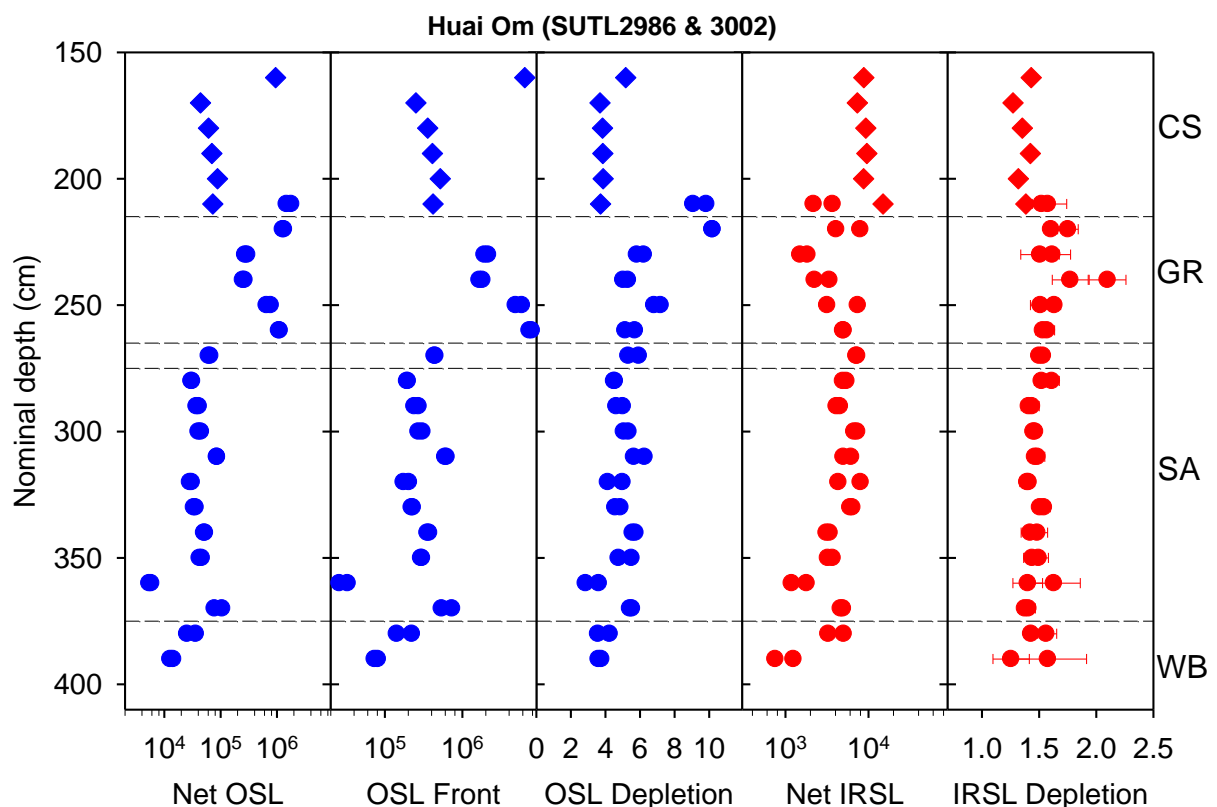


Figure 3.1: Portable OSL measurements for the Huai Om profiles (SUTL2986, diamonds, and SUTL3002, circles). Note that the SUTL2986 data are single measurements of bulk material conducted in petri dishes, whereas the SUTL3002 data are paired aliquots of $<500\mu\text{m}$ material on planchettes. The stratigraphic sequences identified in the field are identified; weathered basement (WB), fine sandy apparent ejecta (SA) with a thin coarse sand layer above it, gravel (GR) and the loess-like cover sands (CS).

Following the measurement of the natural signals, the samples were thermally treated to remove residual signals. Measurements on representative aliquots showed that following this the IRSL signals were indistinguishable from the instrument background and the OSL signals were slightly above background but less than 0.5% of the measured natural signal.

The results of measurements conducted after the addition of a 5Gy beta dose and a short pre-heat are shown in Fig. 3.2 (and tabulated in the Appendix, Table A.2). The IRSL signals were insignificant compared to the instrument background, and are not included in Fig. 3.2. The OSL signals are much larger, with any residual natural signal estimated to be significantly less than 10% of the measured signal.

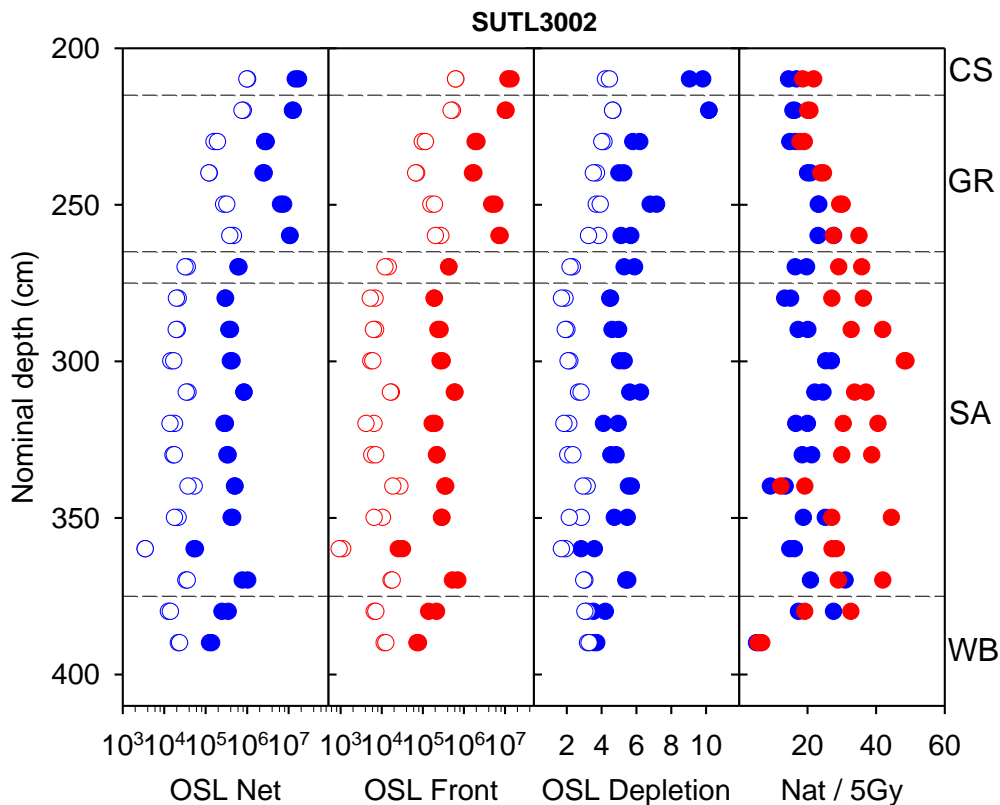


Figure 3.2: Portable OSL measurements showing the OSL net counts, front end and depletion indices for the natural signal (solid circles) and following the 5Gy dose (open circles), and the ratio of counts for the natural to 5Gy signals for the OSL net count (blue) and front end (red) signals.

3.2. Quartz Single Aliquot Regeneration (SAR) and Dose Extension

A procedure to combine Single Aliquot Regeneration (SAR) with dose extension through thermal transfer (see section 2.3.4) was applied to 150-250 μ m quartz grains extracted from the tube samples. Quality parameters for the OSL SAR measurements (sensitivity and change per cycle, recycling ratio, zero cycle and IR percentage) are given in Table 3.1.

Table 3.1: Quality parameters for OSL SAR measurements to 50 Gy

Sample	Sensitivity c Gy ⁻¹	Sensitivity change /cycle %	Zero cycle	Recycling ratio	% IR
SUTL3003	3680 \pm 750	-1.8 \pm 3.9	0.62 \pm 0.05	1.02 \pm 0.04	3.6 \pm 0.1
SUTL3004	2330 \pm 380	-0.4 \pm 3.2	0.38 \pm 0.06	1.06 \pm 0.06	3.6 \pm 0.1
SUTL3005	302400 \pm 28300	-1.1 \pm 2.6	0.76 \pm 0.03	0.96 \pm 0.03	0.0 \pm 0.1

Quality parameters for the dose extension measurements (sensitivity, recycling ratio and zero cycle) are reported in Table 3.2.

Table 3.2: Quality parameters for dose extension from 50-1000 Gy

Sample	Sensitivity c Gy ⁻¹	Zero cycle	Recycling ratio
SUTL3003	73 \pm 30	195 \pm 117	1.08 \pm 0.04
SUTL3004	51 \pm 9	55 \pm 35	1.19 \pm 0.11
SUTL3005	142 \pm 28	58 \pm 32	0.67 \pm 0.02
ID			
SUTL3003	133 \pm 19	-32 \pm 232	1.02 \pm 0.03
SUTL3004	134 \pm 17	65 \pm 230	0.88 \pm 0.01
SUTL3005	61 \pm 10	31 \pm 220	0.97 \pm 0.04
TT-OSL			
SUTL3003	42 \pm 17	246 \pm 72	1.34 \pm 0.07
SUTL3004	17 \pm 4	185 \pm 68	1.05 \pm 0.09
SUTL3005	3350 \pm 550	5220 \pm 920	0.73 \pm 0.01

Dose response curves (Appendix B) were fitted through the measured data, from which the equivalent dose that would produce the measured natural signal was determined for each aliquot, for each of the four measurements. In most cases, a saturating exponential curve was fitted through the data. For SUTL3005, the data for the TL-ramp was consistent with a linear fit over the dose range explored and the isothermal decay data showed a super-linear response for the >500Gy data points, and a linear fit for the 0-200Gy data was used. In all cases, the SAR-OSL measurement saturates at values of the normalised OSL signal below the natural values, and hence the equivalent doses are greater than the saturation dose (>50Gy).

Mean equivalent doses were determined for each sample using an unweighted arithmetic mean, a weighted mean and a robust mean. These are tabulated in Appendix C, with plots of the distributions of equivalent dose. The preferred mean values for each of the measurements are given in Table 3.3. For SUTL3004, the isothermal decay for the natural signal has a significantly different decay rate than those following the laboratory doses, and hence the equivalent doses calculated are unreliable and this measurement has been excluded from the values in Table 3.3.

Table 3.3: Equivalent doses determined for each sample by SAR-OSL and extended dose methods

Sample	Equivalent Dose (Gy)			
	SAR-OSL	TL-ramp	ID	TT-OSL
SUTL3003	> 50	233 ± 8	243 ± 8	115 ± 4
SUTL3004	> 50	108 ± 15	-	92 ± 5
SUTL3005	> 50	88 ± 12	197 ± 9	123 ± 13

3.3. Dose Rates

HRGS results are shown in Table 3.4, both as activity concentrations (i.e. disintegrations per second per kilogram) and as equivalent parent element concentrations (in % and ppm), based in the case of U and Th on combining nuclide specific data assuming decay series equilibrium.

Table 3.4: Activity and equivalent concentrations of K, U and Th determined by HRGS

SUTL no.	Activity Concentration ^a / Bq kg ⁻¹			Equivalent Concentration ^b		
	K	U	Th	K / %	U / ppm	Th / ppm
SUTL3003	276 ± 8	48.1 ± 1.3	46.3 ± 0.7	0.89 ± 0.02	3.89 ± 0.10	11.42 ± 0.18
SUTL3004	46 ± 5	10.6 ± 0.7	11.6 ± 0.6	0.15 ± 0.02	0.85 ± 0.06	2.86 ± 0.14
SUTL3005	106 ± 6	38.5 ± 1.1	27.1 ± 0.6	0.34 ± 0.02	3.12 ± 0.09	6.67 ± 0.15

^aShap granite reference, working values determined by David Sanderson in 1986, based on HRGS relative to CANMET and NBL standards.

^bActivity and equivalent concentrations for U, Th and K determined by HRGS (Conversion factors based on NEA (2000) decay constants): 40K: 309.3 Bq kg⁻¹ % K⁻¹, 238U: 12.35 Bq kg⁻¹ ppmU⁻¹, 232Th: 4.057 Bq kg⁻¹ ppm Th⁻¹

Infinite matrix alpha, beta and gamma dose rates from HRGS are listed for all samples in Table 3.5, together with infinite matrix beta dose rates from TSBC. The gamma spectrometry shows no evidence of disequilibrium in the samples, nor anomalous U:Th ratios, which is supported by the TSBC giving data consistent with the values calculated from the HRGS data. The dry beta dose rates carried forward to calculate effective dose rates are the mean of the HRGS and TSBC values.

Table 3.5: Infinite matrix dose rates determined by HRGS and TSBC

SUTL no.	HRGS, dry ^a / mGy a ⁻¹			TSBC, dry / mGy a ⁻¹
	Alpha	Beta	Gamma	
3003	19.3 ± 0.3	1.63 ± 0.03	1.22 ± 0.02	1.74 ± 0.05
3004	4.5 ± 0.2	0.33 ± 0.02	0.27 ± 0.01	0.63 ± 0.04
3005	13.6 ± 0.3	0.92 ± 0.02	0.76 ± 0.01	0.85 ± 0.04

^abased on dose rate conversion factors in Aikten (1983), Sanderson (1987) and Cresswell et.al. (2018c)

Effective dose rates to the HF-etched 150-250 µm quartz grains are given in Table 3.6 (the mean of the TSBC and HRGS data, accounting for water content and grain size), together with the estimate of the gamma dose rate (HRGS data, accounting for water content), and the total dose rate (the sum of effective beta and gamma dose rates, and the cosmic dose rate). A cosmic dose rate of 0.185 mGy a⁻¹ has been used.

Table 3.6: Effective beta and gamma dose rates following water content correction.

SUTL no.	Water content (%)			Effective Dose Rate / mGy a ⁻¹		
	Received	Saturated	Assumed	Beta ^a	Gamma	Total ^b
3003	20.8	21.7	20 ± 2	1.18 ± 0.05	1.00 ± 0.02	2.36 ± 0.05
3004	4.3	11.1	7 ± 3	0.38 ± 0.04	0.25 ± 0.01	0.82 ± 0.04
3005	12.5	17.6	15 ± 2	0.67 ± 0.02	0.65 ± 0.02	1.51 ± 0.03

^a Effective beta dose rate combining water content corrections with inverse grain size attenuation factors obtained by weighting the 150-250 µm attenuation factors of Mejdahl (1979) for K, U, and Th by the relative beta dose contributions for each source determined by Gamma Spectrometry;

^b includes a cosmic dose contribution determined by the method of Prescott & Hutton (1994)

4. Discussion

For the Huai Om profile (SUTL3002), these materials were presented to the portable instrument in different geometries from early measurements of a higher section of the exposure. Placing the samples as thin layers of $<500\mu\text{m}$ grains on planchettes results in a similar IRSL response to the thicker bulk samples in petri dishes for the samples from equivalent locations. However, for the OSL measurements the planchette geometry results in net signals more than an order of magnitude larger, and faster depletion. Previous measurements (Cresswell et.al. 2019) had indicated that there were two classes of material in the section, a high sensitivity class in the upper layers with lower sensitivity in lower layers. The results of the laboratory profiling reported here indicate that the sand-sized quartz grains in the gravel layer have similar luminescence properties to the lower sensitivity quartz in the cover sands immediately above the gravel. However, the sandy layers below the gravel layer form a third class of materials, with even lower quartz sensitivity, with properties similar to the quartz grains from the weathered basement at the bottom of the profile.

The tube sample from Huai Om (SUTL3003) shows very similar properties to the previously measured sample (SUTL2989) collected approximately 1m further up the profile (Cresswell et.al. 2019). The OSL sensitivity for SUTL3003 is higher ($3680 \pm 750 \text{ c Gy}^{-1}$ cf $1000 \pm 100 \text{ c Gy}^{-1}$), with a correspondingly higher sensitivity for the thermal transfer measurements. The dose rate for SUTL3003 is slightly higher ($2.4 \pm 0.1 \text{ mGy a}^{-1}$ cf $1.9 \pm 0.1 \text{ mGy a}^{-1}$). The equivalent dose from the TL-ramp and ID measurements give a value of $240 \pm 10 \text{ Gy}$, with a lower value from TT-OSL of $115 \pm 4 \text{ Gy}$, inflating these by 20% (following the correction calculated in Cresswell et.al. 2019) gives an age of $120 \pm 10 \text{ ka}$, slightly older than SUTL2989 ($95 \pm 15 \text{ ka}$).

The sample from the granule layer at Pakse (SUTL3004) shows similar luminescence properties to the Huai Om samples, except for the isothermal decay which shows a difference in signal depletion between the natural and artificial doses not observed in other samples. The concentrations of natural radionuclides in this sample are lower, leading to a lower dose rate ($0.82 \pm 0.04 \text{ mGy a}^{-1}$). The equivalent dose from the TL-ramp and TT-OSL give a value of $100 \pm 15 \text{ Gy}$, giving an age of $150 \pm 25 \text{ ka}$.

The breccia sample from Tad Huakhon (SUTL3005) is taken from a layer between the basement and a basalt layer, and shows sensitivities in OSL and TT-OSL two orders of magnitude higher than the lower sand and granule layer samples examined. It is known that heating quartz minerals would normally result in an increase in sensitivity, and thus this higher sensitivity would be consistent with the material being heated by the lava flow above it. The OSL measurements are saturated. The TL-ramp and TT-OSL measurements give an equivalent dose of $100 \pm 20 \text{ Gy}$, with 197 ± 9 from the isothermal decay. The dose rate is $1.51 \pm 0.03 \text{ mGy a}^{-1}$, which would give an age of $80 \pm 20 \text{ ka}$ (TL-ramp and TT-OSL) or $160 \pm 20 \text{ ka}$ (ID). A date for the lava flow would provide an external control to the luminescence dating.

Table 4.1: Summary of dose rates, luminescence properties, equivalent doses and ages for basal samples from five studies of eight sites in Thailand, Laos and Vietnam.

Location	Dose rate (mGy a ⁻¹)	OSL intensity (c Gy ⁻¹)	Equivalent dose (Gy)	Age (ka)	Comment
Khon Kaen, Thailand	1.0 ± 0.1		35 ± 2	35 ± 2	Sanderson et.al. (2001)
Kok Yai, Thailand	0.65 ± 0.03		12.4 ± 2.7	19.2 ± 4.3	Analysis by N. Porat (2017)
Krahad, Thailand	0.67 ± 0.03		5.7 ± 1.0	8.5 ± 1.5	Analysis by N. Porat (2017)
Hue, Vietnam	2.0 ± 0.2	810 ± 90	28 ± 2 (OSL) 200-250 (extended)	14.4 ± 2.1 100-125	Cresswell et.al. (2018a) Cresswell et.al. (2018b)
Kok Yai, Thailand	1.0 ± 0.1	102700 ± 5900	10.7 ± 0.5	10.7 ± 0.5	E _D from SAR-OSL
Huai Om, Thailand 2018	1.9 ± 0.1	1000 ± 100	150 ± 20	80 ± 15	E _D from TL-ramp & TT-OSL, inflated by 20%
2019 [†]	2.4 ± 0.1	3680 ± 750	280 ± 15	120 ± 10	E _D from TL-ramp & ID, inflated by 20%
Sa Kaeo, Thailand	0.5 ± 0.1	89200 ± 4100	4.3 ± 0.1	8.6 ± 0.2	E _D from SAR-OSL
Pakse, Laos [†]	0.8 ± 0.1	2330 ± 380	120 ± 20	150 ± 25	E _D from TL-ramp & TT-OSL, inflated by 20%
Tad Huakhon, Laos [†]	1.5 ± 0.1	302400 ± 28300	120 ± 25	80 ± 20	E _D from TL-ramp & TT-OSL, inflated by 20%

[†] Results reported in this work

5. Conclusions

Studies of samples from cover sands in Thailand and Vietnam have shown two distinct materials present in these formations. Material containing high sensitivity quartz with robust luminescence ages <35ka determined by SAR methods, and material containing lower sensitivity quartz with OSL signals in excess of the saturation limit of the SAR method (~50ka ages for the dose rates typical in these locations). Dose extension methods have been developed to extend the range of equivalent dose determination for these older materials, and have been applied to the lower sections of the cover sands and granule layers beneath them (Cresswell et.al. 2018a, b, 2019). In the work reported here, additional samples from three sites have been analysed to extend the geographical extent of the observations.

These additional samples show similar luminescence characteristics from samples already analysed from equivalent contexts in Thailand and Vietnam, with similar ages determined from the dose extension approach used. The ages determined (100-150ka) are significantly younger than would be expected from the association of these sediments with tektites from an impact event 750-800ka.

References

- Aitken, M.J., 1983, Dose rate data in SI units: PACT, v. 9, p. 69–76.
- Bishop, P., Mitchell, P., Paton, T.R., 1980. The formation of duplex soils on hillslopes in the Sydney Basin, Australia. *Geoderma* 23, 175-189.
- Boonsener, M., Tassanasorn, A., 1983. The geomorphology of Quaternary deposits in Khon Kaen Province, northeastern Thailand. In: Thiramongkol, N., Pisutha-Arnond, V. (Eds), *Proceedings of the First Symposium on Geomorphology and Quaternary Geology of Thailand (October 28-29, 1983)*, Department of Geology Chulalongkorn University, Department of Mineral Resources, and Geological Society of Thailand, pp. 106-111.
- Boonsener, M., 1987. Quaternary geology of Khon Kaen Province, northeastern Thailand. In: Thiramongkol, N. (Ed.), *Proceedings of the Workshop on Economic Geology. Tectonics, Sedimentary Processes and Environment of the Quaternary in Southeast Asia (3-7 February, 1986, Haad Yai, Thailand)*, International Geological Correlations Programme, Dept of Geology Chulalongkorn University, Association of Geoscientists for International Development, pp. 75-85.
- Chalmers, R.O., Henderson, E.P., Mason, B., 1976. Occurrence, distribution, and age of Australian tektites. *Smithsonian Contrib. Earth Sci.* 17, 1-46.
- Chalmers, R.O., Henderson, E.P., Mason, B., 1979. Australian microtektites and the stratigraphic age of the australites: Discussion. *GSA Bull.* 90, 508-510.
- Cresswell, A.J., Sanderson, D.C.W., Carling, P.A., 2018a. Luminescence Profile Measurements on Samples from Vietnam Submitted by P. Carling. SUERC Technical report.
- Cresswell, A.J., Sanderson, D.C.W., Carling, P.A., 2018b, Dose Extension of a Sample at the Base of a Sedimentary Sequence in Vietnam. SUERC Technical Report.
- Cresswell, A.J., Carter, J., Sanderson, D.C.W., 2018c, Dose rate conversion parameters: assessment of nuclear data. *Radiation Measurements* 120, 195-201. doi 10.1016/j.radmeas.2018.02.007
- Cresswell, A.J., Sanderson, D.C.W., Carling, P.A., Darby, S., 2019, SE Asia Agricultural Soils Age Analysis. SUERC Technical Report.
- Darwin, C.R., 1844. Geological observations on the volcanic islands visited during the voyage of H.M.S. Beagle, together with some brief notices of the geology of Australia and the Cape of Good Hope. Being the second part of the geology of the voyage of the Beagle, under the command of Capt. Fitzroy, R.N. during the years 1832 to 1836. Smith Elder and Co., London, pp. 36–39.
- De Dapper, M., 1987. Landform development during the Late Quaternary in the upland of peninsular Malaysia. In: Wezel, F.W., Rau, J.L. (Eds), *Progress in Quaternary Geology of East and Southeast Asia. Proceedings of the CCOP Symposium on Developments in Quaternary Geological Research in E and SE Asia During the Last Decade, (27-30 October, 1986, Bangkok, Thailand)*, CCOP Technical Publication Vol. 18, pp. 109-134.
- Dheeradilok, P., 1987. Review of Quaternary geological mapping and research in Thailand. In: Wezel, F.W., Rau, J.L., (Eds), *Proceedings of the CCOP Symposium on Developments in Quaternary Geological Research in East and Southeast Asia During the Last Decade, 27-30 October, 1986, Bangkok, Thailand.*
- Fleischer, R.L., Price, P.B., Viertl, J.R.M., Woods, R.T., 1969, Ages of Darwin Glass, Macedon Glass, and Far Eastern tektites. *Geochimica et Cosmochimica Acta*, 33, 1071-1074.
- Gentner, W., Storzer, D., Wagner, G.A., 1969, New fission track ages of tektites and related glasses. *Geochimica et Cosmochimica Acta*, 33, 1075-1081.

- Glass, B.P., 1978. Australasian microtektites and the stratigraphic age of the australites. *GSA Bull.* 89, 1455-1458.
- Hoang Ngoc Ky., 1989. The Thu Duc loess formation, a typical aeolian deposit of tropical regions, in ESCAP Secretariat, *Quaternary Stratigraphy of Asia and the Pacific*. IGCP 296 (1989). ESCAP Atlas of Stratigraphy X (Mineral Resources Development Series 60), pp. 100-104.
- Hoang Ngoc Ky., 1994. Stratigraphic correlation of Quaternary transgression and regression deposits in Viet Nam and adjacent countries. In: ESCAP Secretariat, *Quaternary Stratigraphy of Asia and the Pacific*. IGCP 296. ESCAP Atlas of Stratigraphy XIII Mineral Resources Development Series Vol. 63, pp. 141-149.
- Johnson, D.L., 1993. Dynamic denudational evolution of tropical, subtropical and temperate landscapes with three tiered soils: toward a general theory of landscape evolution. *Quaternary International* 17, 67-78.
- Koeberl, C., 1992, Geochemistry and origin of Muong Nong-type tektites, *Geochimica et Cosmochimica Acta*, 56, 1033-1064.
- Lacroix, A., 1935. Les tectites sans formes figurées de l'Indochine. *Comot. Rend. Acad. Sci. Paris*, 200, 2129-2132.
- Löffler, E., Kubiniok, J., 1991. The age and origin of the Yasothon soils and associated gravel deposits. *Journal of the Geological Society of Thailand* 1, 69-74.
- Löffler, E., Kubiniok, J., 1996. landform development and bioturbation on the Khorat plateau, northeast Thailand. *Natural History Bulletin of the Siam Society* 44, 199-216.
- Lovering, J.F., Mason, B., Williams, G. E., McColl, D. H., 1972, Stratigraphical evidence for the terrestrial age of australites, *Journal of the Geological Society of Australia*, 18, 409-418.
- Mejdahl, V., 1979, Thermoluminescence dating: Beta-dose attenuation in quartz grains *Archaeometry*, v. 21, p. 61-72.
- Mizera, J., Řanda, Z., Kameník, J., 2016, On a possible parent crater for Australasian tektites: Geochemical, isotopic, geographical and other constraints. *Earth-Science Reviews* 154, 123–137.
- NEA, 2000, The JEF-2.2 Nuclear Data Library: Nuclear Energy Agency, Organisation for economic Co-operation and Development. JEFF Report, v. 17.
- Nichol, J.E, Nichol, D.W., 2015, Character and provenance of aeolian sediments in northeast Thailand. *Aeolian Research* 19, 5–14.
- Nguyen Duc Tam, 1994. Review of Quaternary geological studies in Vietnam, in ESCAP Secretariat, *Quaternary Stratigraphy of Asia and the Pacific*, IGCP 296. United Nations Mineral Resources Development Series 63, 137-140.
- Porat, N., 2017, Thailand Ages Summary (included as Appendix D to this report).
- Prescott, J.R., and Hutton, J.T., 1994, Cosmic ray contributions to dose rates for luminescence and ESR dating: Large depths and long-term time variations: *Radiation Measurements*, v. 23, p. 497-500.
- Sanderson, D.C.W., 1987, Thermoluminescence dating of vitrified Scottish Forts: Paisley, Paisley college.
- Sanderson, D.C.W., 1988, Thick source beta counting (TSBC): A rapid method for measuring beta dose-rates: *International Journal of Radiation Applications and Instrumentation. Part D. Nuclear Tracks and Radiation Measurements*, v. 14, p. 203-207.
- Sanderson, D.C.W., Bishop, P., Houston, I., Boonsener, M., 2001, Luminescence characterisation of quartz-rich cover sands from NE Thailand. *Quaternary Science Reviews* 20, 893-900.

- Sanderson, D.C.W., and Murphy, S., 2010, Using simple portable OSL measurements and laboratory characterisation to help understand complex and heterogeneous sediment sequences for luminescence dating: *Quaternary Geochronology*, v. 5, p. 299-305.
- Schmidt, G., Zhou, L., Wasson, J.T., 1993. Iridium anomaly associated with the Australasian tektite-producing impact: masses of the impactor and of the Australasian tektites. *Geochim. Cosmochim. Acta* 57, 4851–4859.
- Schnetzler, C.C., Walter, L.S., Marsh, J.G., 1988. Source of the Australasian tektite strewn field: a possible off shore impact site. *Geophys. Res. Lett.* 15, 357–360.
- Shaw, H.F., Wasserburg, G.J., 1982. Age and provenance of the target materials
- Šibrava, V., 1993. Quaternary sequences in Southeast Asia and their regional correlation, in ESCAP Secretariat, *Quaternary Stratigraphy of Asia and the Pacific*. IGCP 296. ESCAP Secretariat, *Quaternary Stratigraphy of Asia and the Pacific*. IGCP 296. ESCAP Atlas of Stratigraphy XII (Mineral Resources Development Series 62), pp. 1-29.
- Sonsuk, M., Hastings, P., 1984. An age for the Yasothon soils series in the Sakhon Nakhon basin. *Journal of the Geological Society of Thailand* VII, 1-11.
- Tamura, T., 1992. Landform Development and Related Changes in the Chi River Basin, Northeast Thailand. *The Science Reports of the Tohoku University*, 7th Series, vol 42, 107-127.
- Udomchoke, V., 1989. Quaternary stratigraphy of the Khorat Plateau area northeastern Thailand. In: Thiramongkol, N. (Ed.), *Proceedings of the Workshop on Correlations of Quaternary Successions in South, East and Southeast Asia (November 21-24, 1988)*, International Geological Correlation Programme, Chulalongkorn University Dept of Geology, UNESCO Regional Office for Science and Technology SE Asia, ESCAP, 69-94.
- Williams, M.A.J., 1978. Termites, soils and landscape equilibrium in the Northern Territory of Australia. In: Davies, J.L., Williams, M.A.J. (Eds.), *Landform Evolution in Australasia*. ANU Press, Canberra, pp. 128-141.

Appendix A: Portable OSL and Laboratory Profiling Data

Table A.1: Measurements of natural luminescence from Huai Om profile (SUTL3002) using the SUERC Portable OSL instrument.

Sample	IRSL		OSL		IRSL:OSL
	Net counts	Depletion index	Net counts	Depletion index	
SUTL3002/1	3690 ± 95	1.52 ± 0.08	17874173 ± 4231	9.07 ± 0.01	0.000 ± 0.001
	2177 ± 107	1.58 ± 0.17	14836387 ± 3856	9.83 ± 0.01	0.000 ± 0.001
SUTL3002/2	4068 ± 96	1.75 ± 0.09	13267962 ± 3646	10.19 ± 0.01	0.000 ± 0.001
	7958 ± 116	1.60 ± 0.05	12697723 ± 3566	10.18 ± 0.01	0.001 ± 0.001
SUTL3002/3	1836 ± 85	1.62 ± 0.16	2717158 ± 1651	5.82 ± 0.01	0.001 ± 0.001
	1505 ± 80	1.51 ± 0.17	2955942 ± 1723	6.22 ± 0.01	0.001 ± 0.001
SUTL3002/4	3378 ± 110	2.10 ± 0.16	2645500 ± 1630	5.30 ± 0.01	0.001 ± 0.001
	2243 ± 90	1.77 ± 0.16	2477917 ± 1577	5.02 ± 0.01	0.001 ± 0.001
SUTL3002/5	3178 ± 89	1.51 ± 0.09	6533947 ± 2559	6.82 ± 0.01	0.000 ± 0.001
	7421 ± 118	1.63 ± 0.06	7727613 ± 2783	7.19 ± 0.01	0.001 ± 0.001
SUTL3002/6	4930 ± 100	1.53 ± 0.07	11160567 ± 3344	5.70 ± 0.01	0.000 ± 0.001
	5015 ± 101	1.57 ± 0.07	10859237 ± 3298	5.15 ± 0.01	0.000 ± 0.001
SUTL3002/7	7135 ± 108	1.50 ± 0.05	613800 ± 787	5.92 ± 0.02	0.012 ± 0.001
	7296 ± 112	1.53 ± 0.05	651650 ± 811	5.32 ± 0.02	0.011 ± 0.001
SUTL3002/8	4914 ± 98	1.52 ± 0.06	302020 ± 554	4.54 ± 0.02	0.016 ± 0.001
	5407 ± 102	1.61 ± 0.06	309867 ± 562	4.50 ± 0.02	0.017 ± 0.001
SUTL3002/9	4124 ± 94	1.41 ± 0.07	371928 ± 614	4.63 ± 0.02	0.011 ± 0.001
	4523 ± 96	1.44 ± 0.06	407132 ± 643	5.00 ± 0.02	0.011 ± 0.001
SUTL3002/10	7303 ± 109	1.46 ± 0.05	403264 ± 639	5.06 ± 0.02	0.018 ± 0.001
	6717 ± 107	1.45 ± 0.05	444917 ± 671	5.32 ± 0.02	0.015 ± 0.001
SUTL3002/11	6169 ± 105	1.46 ± 0.05	857674 ± 929	5.65 ± 0.02	0.007 ± 0.001
	4987 ± 103	1.49 ± 0.06	860975 ± 932	6.26 ± 0.02	0.006 ± 0.001
SUTL3002/12	4332 ± 96	1.40 ± 0.06	306233 ± 558	4.98 ± 0.02	0.014 ± 0.001
	8027 ± 115	1.41 ± 0.04	285006 ± 540	4.13 ± 0.02	0.028 ± 0.001
SUTL3002/13	6374 ± 107	1.54 ± 0.05	357098 ± 603	4.56 ± 0.02	0.018 ± 0.001
	6019 ± 105	1.51 ± 0.05	335280 ± 584	4.86 ± 0.02	0.018 ± 0.001
SUTL3002/14	3399 ± 92	1.42 ± 0.08	507144 ± 716	5.57 ± 0.02	0.007 ± 0.001
	3125 ± 91	1.48 ± 0.09	527504 ± 730	5.73 ± 0.02	0.006 ± 0.001
SUTL3002/15	3239 ± 90	1.50 ± 0.09	422683 ± 654	5.50 ± 0.02	0.008 ± 0.001
	3692 ± 93	1.44 ± 0.07	460407 ± 683	4.76 ± 0.02	0.008 ± 0.001
SUTL3002/16	1191 ± 78	1.63 ± 0.23	58335 ± 252	3.61 ± 0.04	0.020 ± 0.001
	1796 ± 80	1.40 ± 0.13	53912 ± 242	2.86 ± 0.03	0.033 ± 0.001
SUTL3002/17	4632 ± 98	1.41 ± 0.06	1062851 ± 1034	5.42 ± 0.01	0.004 ± 0.001
	4920 ± 98	1.38 ± 0.06	778803 ± 886	5.53 ± 0.02	0.006 ± 0.001
SUTL3002/18	5020 ± 98	1.43 ± 0.06	359671 ± 604	4.24 ± 0.02	0.014 ± 0.001
	3278 ± 91	1.56 ± 0.09	253443 ± 509	3.57 ± 0.02	0.013 ± 0.001
SUTL3002/19	1245 ± 78	1.26 ± 0.16	143114 ± 384	3.60 ± 0.02	0.009 ± 0.001
	755 ± 76	1.58 ± 0.34	127304 ± 364	3.76 ± 0.03	0.006 ± 0.001

Table A.2: Measurements of luminescence from Huai Om profile (SUTL3002) following 5Gy dose, using the SUERC Portable OSL instrument.

Sample	IRSL		OSL		IRSL:OSL
	Net counts	Depletion index	Net counts	Depletion index	
SUTL3002/1	112 ± 69	2.20 ± 3.37	1086696 ± 1098	4.41 ± 0.01	0.000 ± 0.001
	174 ± 72	2.63 ± 2.97	1015036 ± 1011	4.48 ± 0.01	0.000 ± 0.001
SUTL3002/2	336 ± 70	1.63 ± 0.74	834020 ± 917	4.67 ± 0.01	0.000 ± 0.001
	121 ± 71	2.78 ± 4.66	773151 ± 883	4.66 ± 0.01	0.000 ± 0.001
SUTL3002/3	125 ± 70	0.56 ± 0.71	163055 ± 410	4.16 ± 0.03	0.000 ± 0.001
	97 ± 71	-25.25 ± 314.43	197162 ± 450	4.04 ± 0.02	0.000 ± 0.001
SUTL3002/4	74 ± 70	2.70 ± 7.09	125930 ± 362	3.74 ± 0.03	0.000 ± 0.001
	263 ± 71	1.48 ± 0.84	122878 ± 358	3.55 ± 0.03	0.002 ± 0.001
SUTL3002/5	116 ± 70	-6.27 ± 14.03	278758 ± 533	3.72 ± 0.02	0.000 ± 0.001
	129 ± 70	0.48 ± 0.63	331587 ± 580	3.95 ± 0.02	0.000 ± 0.001
SUTL3002/6	215 ± 71	0.89 ± 0.59	480375 ± 697	3.86 ± 0.01	0.000 ± 0.001
	147 ± 71	1.07 ± 1.04	391144 ± 630	3.28 ± 0.01	0.000 ± 0.001
SUTL3002/7	224 ± 71	0.41 ± 0.34	37006 ± 205	2.35 ± 0.03	0.006 ± 0.002
	12 ± 70	0.71 ± 8.74	32742 ± 195	2.22 ± 0.03	0.000 ± 0.002
SUTL3002/8	-24 ± 72	-0.43 ± 1.32	22372 ± 165	1.93 ± 0.03	-0.001 ± 0.003
	-79 ± 70	1.08 ± 1.93	20330 ± 159	1.72 ± 0.03	-0.004 ± 0.003
SUTL3002/9	82 ± 71	1.83 ± 3.59	21349 ± 162	2.04 ± 0.03	0.004 ± 0.003
	-107 ± 70	-0.15 ± 0.40	20105 ± 158	1.95 ± 0.03	-0.005 ± 0.004
SUTL3002/10	78 ± 70	-4.55 ± 10.28	14859 ± 141	2.21 ± 0.05	0.005 ± 0.005
	331 ± 70	1.12 ± 0.48	17479 ± 150	2.11 ± 0.04	0.019 ± 0.004
SUTL3002/11	393 ± 71	1.26 ± 0.46	38482 ± 208	2.70 ± 0.03	0.010 ± 0.002
	202 ± 71	1.93 ± 1.58	34939 ± 200	2.85 ± 0.04	0.006 ± 0.002
SUTL3002/12	87 ± 70	-0.1 ± 0.51	18303 ± 152	2.15 ± 0.04	0.005 ± 0.004
	66 ± 70	2.00 ± 5.02	14148 ± 137	1.87 ± 0.04	0.005 ± 0.005
SUTL3002/13	110 ± 69	1.39 ± 1.82	16708 ± 177	2.09 ± 0.04	0.007 ± 0.004
	-43 ± 70	1.39 ± 4.73	18017 ± 152	2.37 ± 0.05	-0.002 ± 0.004
SUTL3002/14	280 ± 70	1.06 ± 0.53	54399 ± 244	3.20 ± 0.03	0.005 ± 0.001
	50 ± 70	0.25 ± 1.27	38652 ± 209	2.96 ± 0.04	0.001 ± 0.002
SUTL3002/15	118 ± 71	-24.6 ± 244.98	22294 ± 165	2.86 ± 0.05	0.005 ± 0.003
	136 ± 71	0.64 ± 0.71	18178 ± 152	2.18 ± 0.04	0.007 ± 0.004
SUTL3002/16	150 ± 69	0.60 ± 0.61	3575 ± 92	1.96 ± 0.11	0.042 ± 0.019
	90 ± 70	0.53 ± 0.94	3594 ± 91	1.72 ± 0.09	0.025 ± 0.019
SUTL3002/17	140 ± 69	0.97 ± 0.96	34144 ± 197	3.07 ± 0.04	0.004 ± 0.002
	241 ± 72	2.65 ± 2.17	37061 ± 206	3.00 ± 0.04	0.007 ± 0.002
SUTL3002/18	0 ± 73	-1.00 ± 2.09	12964 ± 135	3.19 ± 0.09	
	-8 ± 72	-0.86 ± 1.14	14477 ± 141	3.07 ± 0.08	-0.001 ± 0.005
SUTL3002/19	20 ± 69	-0.39 ± -1.58	22466 ± 166	3.22 ± 0.06	0.001 ± 0.003
	60 ± 71	0.67 ± 1.68	24115 ± 170	3.31 ± 0.06	0.002 ± 0.003

Appendix B: Dose response curves

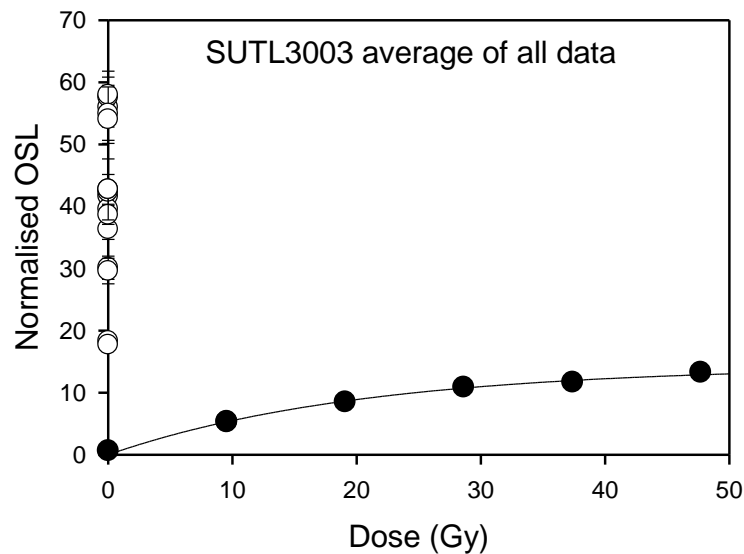


Figure B.1: Dose response curve for OSL SAR measurements on SUTL3003, average of 16 aliquots, with natural signals indicated by open symbols on the left hand axis.

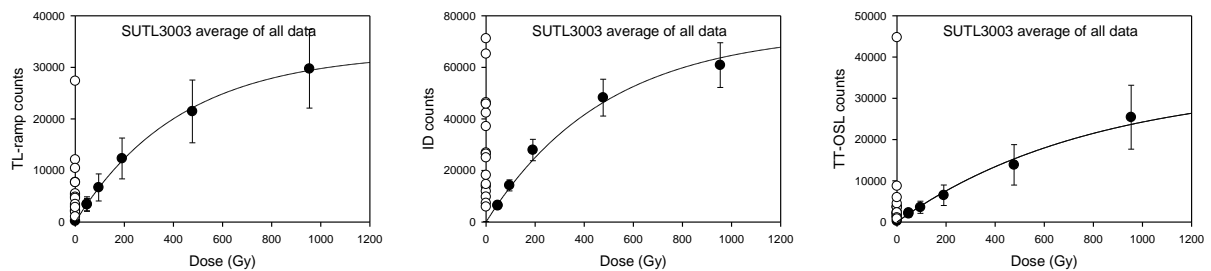


Figure B.2: Dose response curves for dose extension measurements on SUTL3003, average of 16 aliquots, for the TL-ramp (left), isothermal decay (centre) and TT-OSL (right), with natural signals indicated by open symbols on the left hand axes.

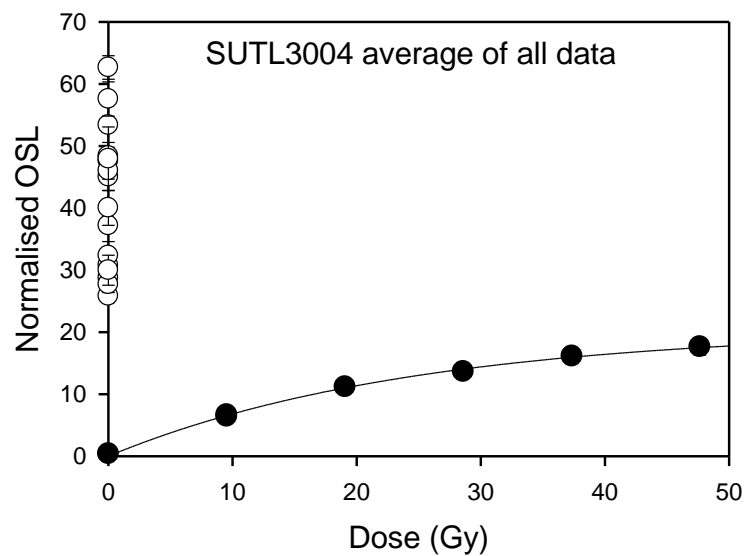


Figure B.3: Dose response curve for OSL SAR measurements on SUTL3004, average of 16 aliquots, with natural signals indicated by open symbols on the left hand axis.

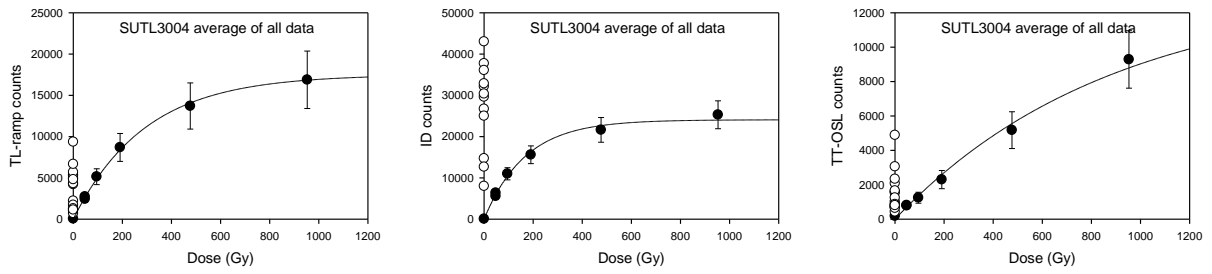


Figure B.4: Dose response curves for dose extension measurements on SUTL3004, average of 16 aliquots, for the TL-ramp (left), isothermal decay (centre) and TT-OSL (right), with natural signals indicated by open symbols on the left hand axes.

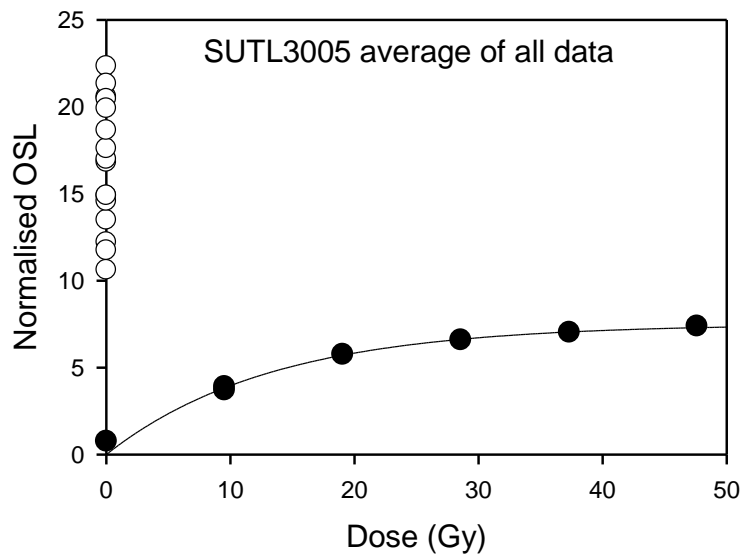


Figure B.5: Dose response curve for OSL SAR measurements on SUTL3005, average of 16 aliquots, with natural signals indicated by open symbols on the left hand axis.

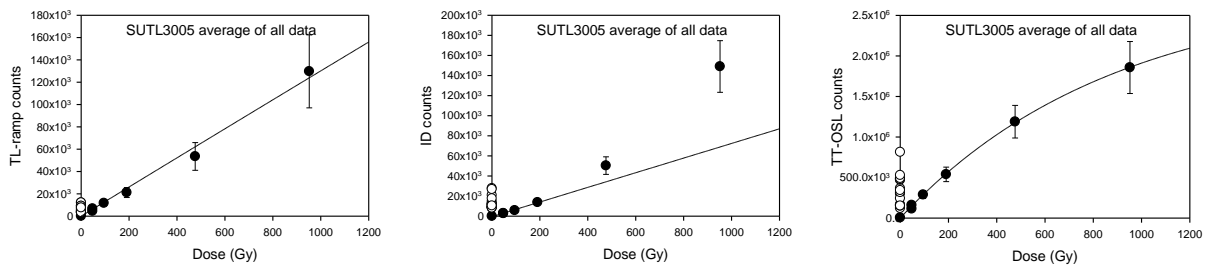


Figure B.6: Dose response curves for dose extension measurements on SUTL3005, average of 16 aliquots, for the TL-ramp (left), isothermal decay (centre) and TT-OSL (right), with natural signals indicated by open symbols on the left hand axes.

Appendix C: Dose distributions

Table C.1: Mean equivalent doses determined by OSL SAR measurements (0-50Gy), preferred value in bold.

Sample	Description of distribution	Mean Equivalent Doses (Gy)		
		Mean	Weighted mean	Robust mean
SUTL3003	Natural counts for all aliquots exceed signal from 50Gy	> 50Gy		
SUTL3004	Natural counts for all aliquots exceed signal from 50Gy	> 50Gy		
SUTL3005	Natural counts for all aliquots exceed signal from 50Gy	> 50Gy		

Table C.2: Mean equivalent doses determined by TL-ramp measurements (0-1000Gy), preferred value in bold.

Sample	Description of distribution	Mean Equivalent Doses (Gy)		
		Mean	Weighted mean	Robust mean
SUTL3003	Two peaks in pdf, one at ~65Gy and second at ~190Gy with tail to high dose	356 ± 133	85 ± 3	233 ± 8
SUTL3004	Excludes 280°C PH group. Broad peak in pdf at ~100Gy with small shoulder at ~200Gy	108 ± 15	98 ± 8	104 ± 6
SUTL3005	Very broad peak in pdf at ~90Gy	88 ± 12	61 ± 11	85 ± 6

Table C.3: Mean equivalent doses determined by ID measurements (0-1000Gy), preferred value in bold.

Sample	Description of distribution	Mean Equivalent Doses (Gy)		
		Mean	Weighted mean	Robust mean
SUTL3003	Broad pdf distribution with peaks at ~200Gy and ~310Gy	318 ± 33	243 ± 8	300 ± 4
SUTL3004	Excludes 280°C PH group. Means of 7 non-saturating aliquots very poorly defined, pdf forms a very broad peak.	653 ± 151	310 ± 74	488 ± 126
SUTL3005	Broad peak in pdf at ~190Gy with tail to high dose	293 ± 35	197 ± 9	287 ± 9

Table C.4: Mean equivalent doses determined by TT-OSL measurements (0-1000Gy), preferred value in bold.

Sample	Description of distribution	Mean Equivalent Doses (Gy)		
		Mean	Weighted mean	Robust mean
SUTL3003	Broad peak in pdf centred at ~110Gy with shoulder at ~200Gy	129 ± 9	115 ± 4	125 ± 2
SUTL3004	Broad peak in pdf centred at ~100Gy	138 ± 19	92 ± 5	128 ± 5
SUTL3005	Multiple peaks in pdf between ~50Gy and ~220Gy, largest peak at ~120Gy.	123 ± 13	87 ± 2	122 ± 4

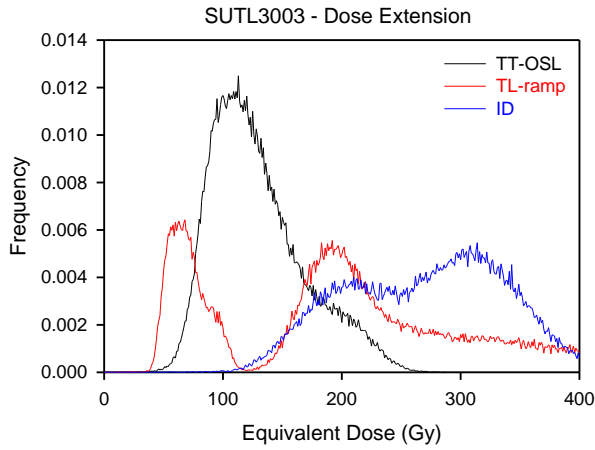


Figure C.1: Probability Density Function for the three measurements of thermally transferred signals for SUTL3003.

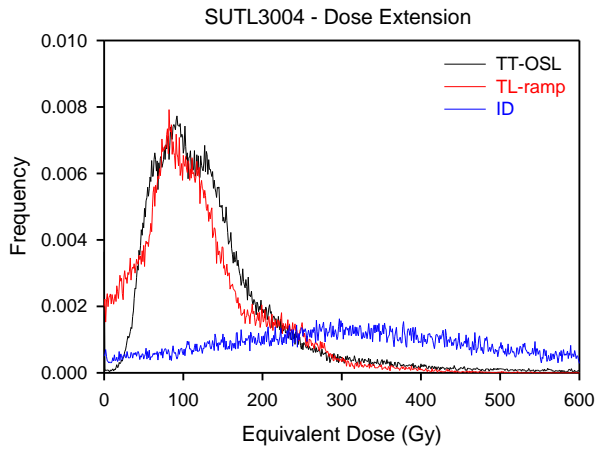


Figure C.2: Probability Density Function for the three measurements of thermally transferred signals for SUTL3004.

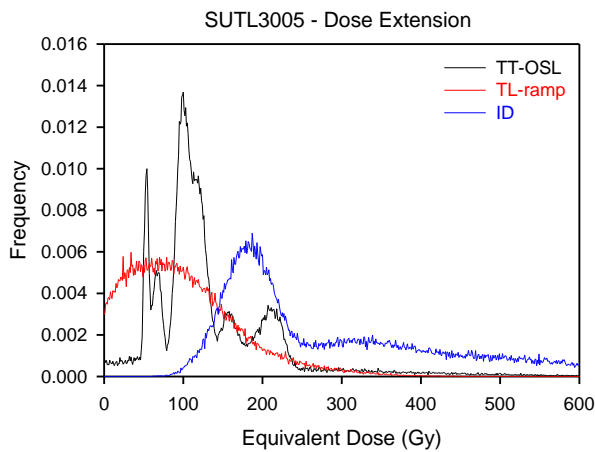


Figure C.3: Probability Density Function for the three measurements of thermally transferred signals for SUTL3004.